# Gemini Multiobject Spectrograph GMOS: integration and tests

David Crampton*, J.M. Fletcher, I. Jean, R. Murowinski, K. Szeto

National Research Council of Canada, 5071 West Saanich Rd., Victoria, BC, V8X 4M6, Canada

C. Dickson, I. Hook, K. Laidlaw, T. Purkins

Astronomy Technology Centre, Blackford Hill, Edinburgh EH9 3HJ, Scotland

J.R. Allington-Smith, R. L. Davies

Dept. of Physics, South Road, Durham University, Durham DH1 3LE, UK

## ABSTRACT

The Gemini Multiobject Optical Spectrographs (one each for Gemini North and South) were designed to exploit the exceptional image quality anticipated from both the active and adaptive optics systems. High mechanical stability and repeatability and efficient reconfiguration and calibration were emphasized in the design, as well as the usual requirements of obtaining excellent image quality, high optical throughput and low optical distortion. In addition, an active flexure compensation system is used to assist in achieving a primary goal of attaining velocity accuracies of 2 km/s per spectrum in multiobject mode at the highest spectral resolution (R = 10,000). Although the field is modest (nominal size for multi-slits is 5.5' square), small pixels (0.07" per pixel) are used to fully sample images as small as 0.2" and 28.3 million pixels will be recorded by the detector mosaic which consists of three 2048 * 4608 EEV CCDs. In this paper, results from extensive tests made during integration and testing of GMOS N components demonstrate that the design requirements are being met

**Keywords:** Spectrograph, astronomical instrumentation, flexure

## 1. INTRODUCTION

The Gemini telescopes are optimized to deliver the best possible images and also the best possible infrared performance from the Mauna Kea and Cerro Pachon sites. Partly as a result of optimization for the IR, and partly due to budget constraints, there is only one focus on each telescope, at a focal ratio of f/16. A consequence of this choice is that, for practical (mostly size) reasons, the field delivered to instruments like GMOS is limited to a diameter of 7 arcmin. Hence GMOS cannot be an extremely widefield spectrograph and so it was designed instead to exploit the excellent anticipated image quality and optimized for precise one-dimensional multiobject spectroscopy and two-dimensional integral field spectroscopy. At Mauna Kea the median and $10^{th}$ percentile seeing images are $0.''4$ and $0.''25$ (FWHM) respectively. The Gemini telescopes are designed so as not to degrade the best natural images by more than 15% and, indeed, early results indicate that this will be achieved[1]. In turn, the GMOS spectrographs are designed so as not to degrade the best images delivered by the telescope by more than 10%. Comprehensive overviews of the GMOS designs are given by Davies et al., 1996[2] and Murowinski et al., 1997[3]. In multiobject mode, several hundred targets in a 5.5 x 5.5 arcmin field can be observed simultaneously. The integral field unit is designed for 2-D spectroscopy of a 5" x 7" area with $0.''2$ sampling.

In order to adequately sample the best natural seeing images and also images produced by the Gemini adaptive optics system, the pixel scale at the focus of the spectrograph was chosen to be $0.''07$ per 13.5 micron pixel. This fine scale and correspondingly narrow slit widths that are possible also permit relatively high spectral resolutions (up to R = 10,000) to be achieved with gratings of diameter of only ~100mm. This relatively small pupil size, combined with a compact optical design (for example three lens groups are used in the collimator to reduce its length), lead to a compact instrument designed to achieve a velocity precision, per exposure, of < 2km/s for objects throughout the field. The latter specification is derived

* Email: David.Crampton@nrc.ca

from the desire to enable scientific projects requiring precise velocity measurements of hundreds of objects simultaneously. For example, the velocities of large samples of stars in dwarf galaxies are required with ~2km/s precision in order that accurate determinations of their dynamical structure and estimates of their dark matter content can be made.

A further consequence of the expected good images delivered by the telescope, and the anticipated narrow slit widths, is that an atmospheric dispersion compensator (ADC) becomes essential for observations at any substantial airmass. Furthermore, a corrector is incorporated into the ADC to partially flatten the telescope focal plane so that a planar slit mask can be used.

The GMOS instruments can either be mounted on the upward-looking or side-looking ports of the Gemini cassegrain support structure and hence must meet their performance specifications in virtually any orientation. Components for each of the GMOS' were designed and built by teams in Durham, Edinburgh and Victoria, and the CCD detector mosaic was integrated into the dewar at NOAO. The sharing of effort among these four establishments required that individual modules be rigorously tested to ensure that their performance met the specifications at all orientations (gravity vectors) and anticipated operating temperatures (from room temperature to –10C). After testing, the modules are being brought together and integrated, together with their software, at Edinburgh. Final testing of the completed instrument is just beginning; here we report results of the component tests.

## 2. RESULTS OF TESTS OF IMAGE QUALITY AND TRANSMISSION

The optical design had to simultaneously satisfy exacting constraints on image quality at all locations in the field in both imaging and spectroscopic configurations at all wavelengths from 370 to 1100nm, maintain very high transmission, with very low distortion and minimal parasitic light. Once it was realized that extension into the non-thermal infrared could be obtained at little expense, the optimization was extended to 1600nm (although there are currently no plans to utilize this feature). To achieve all these specifications a design by C. Morbey composed of six groups of lenses was adopted, with each group comprising several elements including several large pieces of calcium fluoride. Due to production difficulties, the latter proved to be the most difficult to procure on schedule. Because of the mandated requirement to survive and operate over a considerable temperature range, special attention was paid to the mechanical mounting of the optics, especially since the coefficients of thermal expansion of the (sizable) refractive elements differ considerably. Rather than being cemented together, elements in each group are coupled together with oil which, in turn, has a reservoir designed to accommodate volume changes due to both temperature and pressure variations. Furthermore the individual lens elements are mounted to metal rings which have similar coefficients of thermal expansion as the glass itself. Figure 1 shows some of the elements that have been assembled into lens groups in preparation for installation into the lens barrel at the rear in the photograph.

Fig. 1: Three lens groups are shown in the foreground, with a barrel behind. Each group is composed of several glass elements that are attached to metal rings by thin fingers. The gaps between lens elements are filled with an oil couplant. The exterior surfaces of lenses in each group are coated with an AR coating of Mg F and sol-gel.

### 2.1. Results of Image Quality tests

As mentioned previously, the primary optical specification that GMOS is attempting to achieve in all modes is to not degrade the on-axis images delivered by the telescope by more than 10%. The fact that GMOS will likely be used in conjunction with Altair, the Gemini adaptive optics system, is added incentive to realize the best possible images. All of the optics for GMOS N have now been assembled and mounted in their barrels (an example is shown in Fig 1) and measurements of the actual image quality in terms of 50% and 85% encircled energy diameters through the complete optical system have been made. The results are shown, compared with the specifications (lines), in Figure 2. Overall the image quality is excellent, meeting the specifications over essentially the entire wavelength range. The same is true off-axis as well. Tests at –7C confirm that the image quality is identical to that at room temperature.

Fig. 2: The 50% and 85% encircled energy diameters (points) compared with specifications (lines) at various wavelengths.

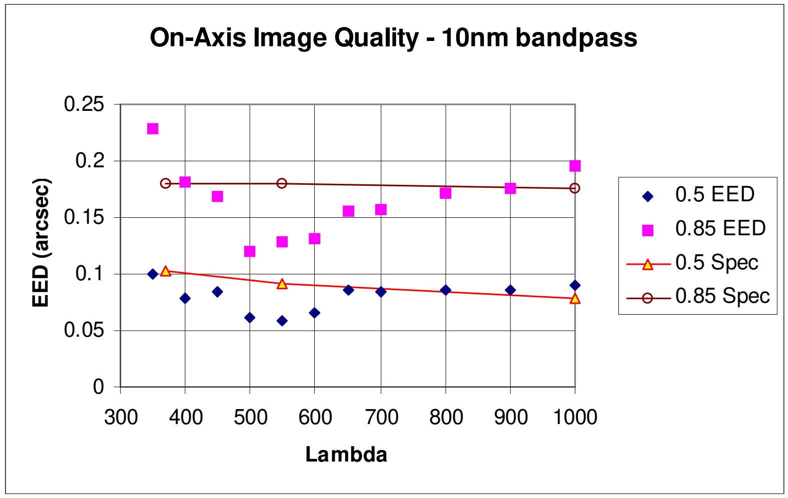


### 2.2. Measurements of Optical Throughput

As shown in Figure 3, the overall transmission of the optical system is extremely good, thanks to selection of glasses with excellent transmission and to the development of superb sol-gel anti-reflection coatings by J. Stilburn[4]. The transmission of the refractive elements is above 80% for wavelengths >700nm and above 70% over most of the remainder. This is almost precisely that predicted for a perfect system. Considering that there are 14 air-glass surfaces on six lens groups containing a total of 19 lens and one (powered) window that will form part of the dewar, this transmission is excellent.

Fig. 3: Measurements of the transmission through all the refractive elements in the GMOS spectrograph, including the window of the CCD dewar.

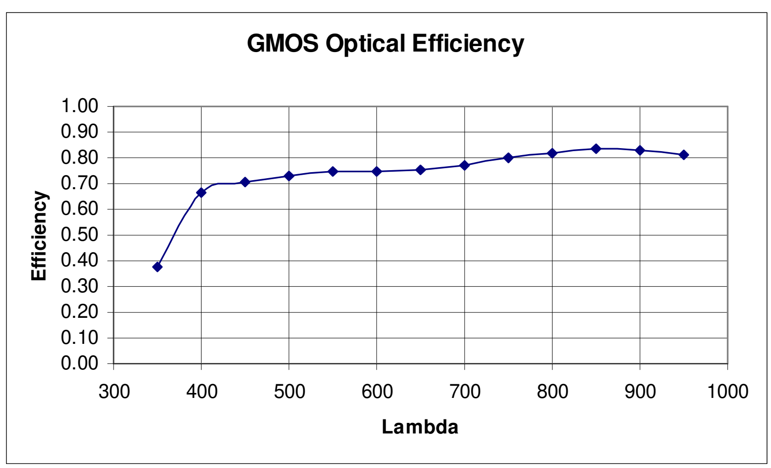

## 3. RESULTS OF TESTS OF MECHANICAL STABILITY AND FLEXURE

One of the primary specifications of the GMOS spectrographs is that the overall system, from the location of the input focal plane to the detector, be mechanically rigid and stable. The main drivers for the precise specifications are the requirement to achieve a velocity precision of 2km/sec (at the highest spectral resolutions) for nominal one hour exposures on individual targets, and the desire to minimize the number of calibration exposures required to achieve good flat-field (including CCD fringing) and wavelength calibrations. In order to realize these goals, the overall mechanical structure was designed so that flexure could be easily modeled and optimized in the design stage (e.g., simple elements like struts were used where possible), and open-loop flexure control was included (by moving the CCD detector focal plane within the dewar). Finite element analyses of major components of the spectrograph indicate that it should be possible to control the overall flexure of this two tonne, two metre scale instrument to meet the scientific requirements. Thus far our tests indicate that the actual performance of each major sub-assembly is very close to predictions. Likewise, tests of the flexure control system under operating conditions demonstrate that it also is performing approximately as expected. In addition to flexure control within the instrument, possible flexure between the telescope guiding system (derived from the so-called peripheral wavefront sensors) and the spectrograph input focal plane will be eliminated through use of another guider (the on-instrument wavefront sensor, OIWFS) which is located immediately in front of the latter. Hence the position of the OIWFS must remain fixed in a stable location with respect to the focal plane, typically a multi-slit mask or an integral field unit. A schematic of the spectrograph with major sub-assemblies identified is shown in Figure 4.

Fig. 4: Schematic view of the GMOS spectrograph (without enclosure panels and electronic racks) as it will look attached to the instrument support structure.

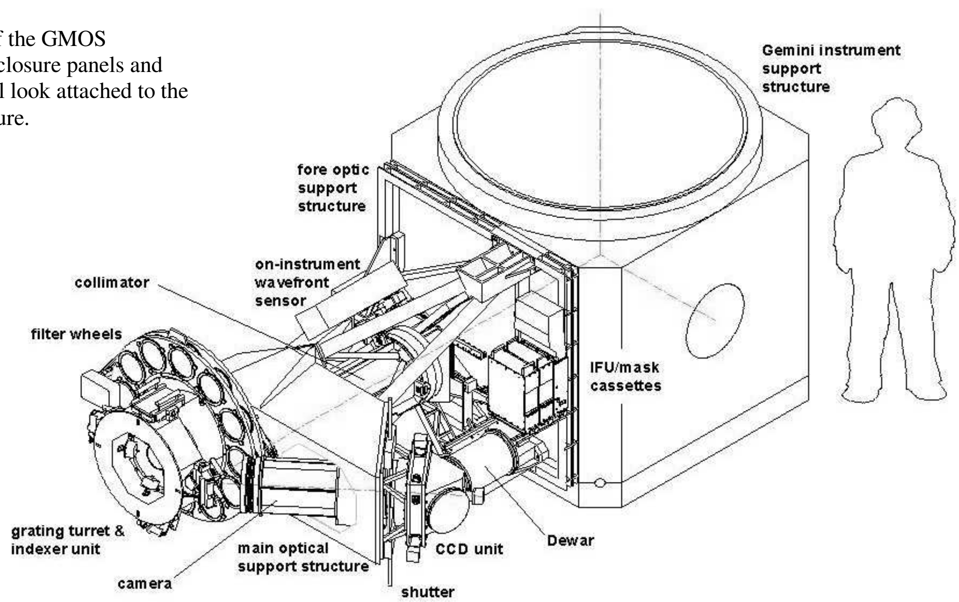


In order to realize the overall stability required to achieve the primary scientific goals of the instrument, an error budget was developed for the various contributing components as shown in Table 1. In turn, each of these is further broken down into maximum allowable contributions for its subcomponents. For example, the slit-spectrograph displacement includes allowance for unmodellable contributions from both the main optics support structure and the fore-optic support structure. A more comprehensive discussion of the error budget is given by Szeto et al. (1998) [5]

Table 1: Overall error budget to achieve stability specification

| Item | Allocation |
| --- | --- |
| Pre focal plane assembly: total | 1.4 µm/hr at detector |
| ADC image distortion contribution | 0.9 µm/hr at detector |
| OIWFS contribution | 0.9 µm/hr at detector |
| Temperature effects on focal plane | 2.0 µm/hr at focal plane |
| Post focal plane assembly: total | 2.8 µm/hr at detector |
| Slit-spectrograph displacement | 0.7 µm/hr |
| Collimator assembly | 1.1 µm/hr at detector |
| Grating assembly | 1.5 µm/hr at detector |
| Camera assembly | 1.5 µm/hr at detector |
| Dewar assembly | 1.1 µm/hr |
| Temperature variation: total (image motion due to plate scale changes) | 0.5 µm/hr at detector |
| Overall stability specification | 3.1 µm/hr for an image on the detector focal surface |

All of the sub-assemblies are being rigorously tested to ensure that the final instrument attains the overall specification. Results from some of these tests are described in the following sections.

### 3.1. Tests of the On-Instrument Wavefront Sensor

Details of the optical and mechanical design of the GMOS OIWFS are given by Roberts et al.[6] The basic requirements of the OIWFS are:

- Patrol more than 50% of the 7 arcmin diameter field to locate a suitable guide star
- Determine tip/tilt and focus information from the guide star and relay that to the telescope control system, including the active and adaptive optic systems.
- Vignette at most 5% of the GMOS input field
- Contribute less than 2.05 microns per hour of guide star positional error at the telescope focal plane regardless of the gravity vector.

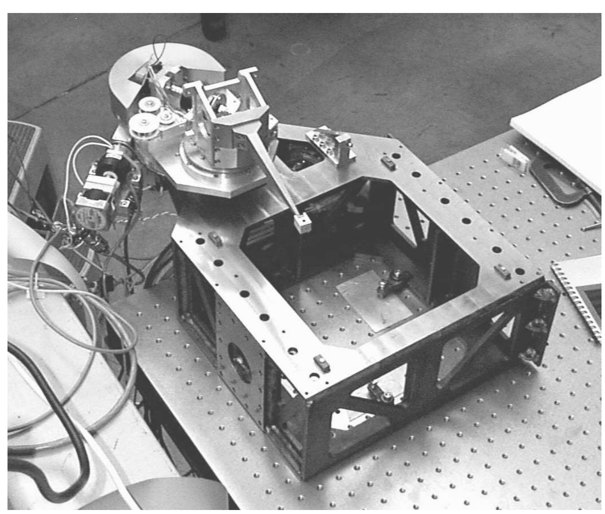

Fig. 5: An early picture of the OIWFS during bench testing. The 5.5 arcminute science field is delineated by the square area in the center. The pick-off mirror at the tip of the probe can reach into beyond the centre of the field and patrol somewhat more than a quadrant of the 7 arcmin diameter field relayed by the fold mirror in the instrument support structure. The probe mechanism is counterweighted by the semi-circular mass at the top of the photograph.

Rigorous tests of the repeatability of positioning the OIWFS probe at varying gravity vectors and at temperatures from –10C to +20C have been carried out, using its own 2x2 Shack-Hartmann sensor to determine its location. Similarly, the flexure between the probe and a hole located at the centre of the slit mask has been measured under the same gravity vector and temperature conditions. The results are excellent. An example is shown in Figure 6. The graph shows the difference between the mask position and the reported OIWFS position as the instrument is tipped over from upward-looking to downward-looking (which is greater than our operational range). During any 15 deg change (maximum for a one hour exposure) the positional change is typically less than 15 mas, only 6% of the diameter of the best images anticipated (0.25”). Similar values were recorded for the displacement between the OIWFS probe and a mockup of the IFU. Thus it is expected that the OIWFS will be able to accurately maintain the positions of objects within slits or within 0.2” IFU elements.

Fig 6: Difference between a fiducial position on the mask and the OIWFS position at gravity vectors from 0 (downward looking) to 180 (upward looking) and back again in 30deg intervals.

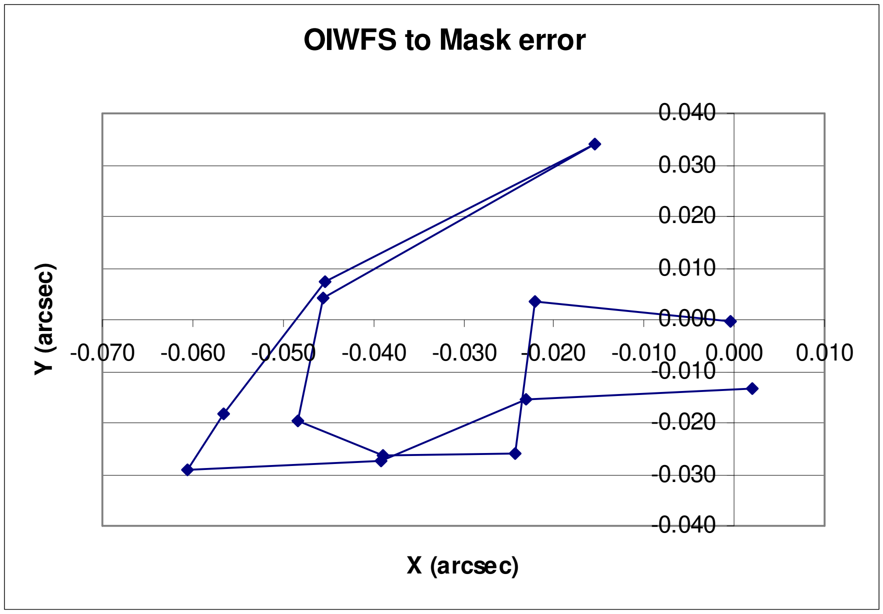


### 3.2. Tests of Mask and IFU insertion

Slit masks and integral field units (IFUs) must also be inserted into the telescope focal plane in a precise and repeatable way and maintained in a fixed position throughout exposures, nominally assumed to be of one hour duration. Since the masks and IFUs have very different mass, the latter activate much stronger spring systems to maintain their position. Tests of the accuracy of repositioning the masks and IFUs, and of their stability once inserted, have been carried out in different gravity vectors. The results are excellent. In fact, no motion at all was detectable at sub-micron level accuracy during the preliminary tests. Similarly, the repeatability of re-inserting masks was better than the 5µm resolution of the measuring equipment. More extensive tests will be made after the unit is integrated into the whole spectrograph assembly.

### 3.3. Tests of Grating assembly

Preliminary measurements of the positioning accuracy and repeatability of the grating mounts have been made. The gratings can be driven to a new location with an accuracy of about 0.025deg but, once there, they can be repositioned with an accuracy some 40X better. The latter is well within our specifications. Measurements of the stability of the grating mounts and the whole grating turret will be carried out after the whole spectrograph is mounted on the flexure testing facility.

### 3.4. Tests of the Translation Stage for the CCD Mosaic

Since some flexure in a large two tonne instrument like GMOS is inevitable, an open-loop flexure control system has been incorporated. The gravity vector and temperatures of GMOS components will be monitored and used to predict image motion as seen at the detector. The CCD mounting assembly has been designed in such a way that the CCD mosaic can be moved in all three axes to correct for the predicted flexure and focus changes. Details of the elegant design are given by P. Hastings[7]. Motions of up to 3.8mm are provided in the focus direction and 0.3mm in each of the orthogonal translational directions. A lever system enables a resolution of 0.4 microns per motor step to be realized. A photograph of the completed stage for GMOS N is shown in Figure 7.

Fig 7: The CCD translation stage. The CCD mosaic is attached to the octagonal plate in the centre of the photo. The two motors that are visible are used to translate the mosaic in X and Y to compensate for flexure of the GMOS instrument

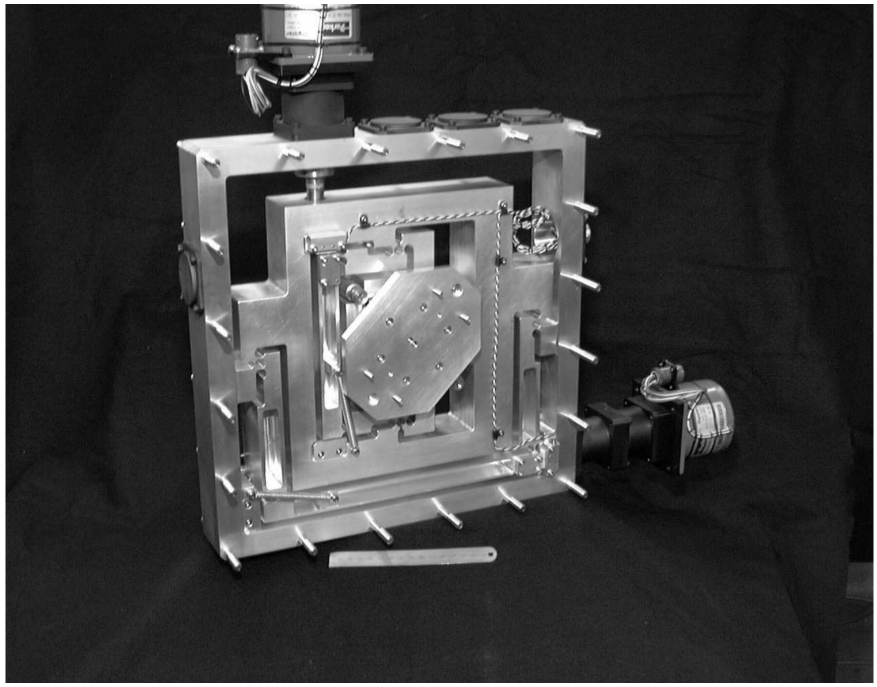

The CCD mosaic has been mounted on the translation stage and integrated with the dewar assembly. Extensive tests of the whole CCD assembly are currently underway. These include characterizing motions of reference images on the CCDs as a result of varying gravity vectors, coupling between motions in any of the orthogonal directions, effects due to temperature variations, etc. These tests are still in progress; the results of one such series designed to characterize the interactions between motions of the CCD detector are shown in Figure 8. In this series, the measurements show how the position of an image varies in X as the CCD assembly is moved in Y by 160µm (~12 pixels) and back again. In actual practice, any translations required to compensate for flexure during an exposure will be much smaller than this, and lookup tables will be used to remove any excursions that would negatively impact on the scientific objectives. Complete characterization of all such motions will be modeled and used to compute precise corrections in all three axes to achieve the required flexure compensation. At this stage, it is unclear what the magnitude of flexure compensation corrections will be under normal operating conditions during a one hour exposure, and so it is not yet possible to be certain that the required specifications are being met. However, the mechanism is now sufficiently well characterized through these extensive tests to show where potential problem areas are and how to improve on them if necessary.

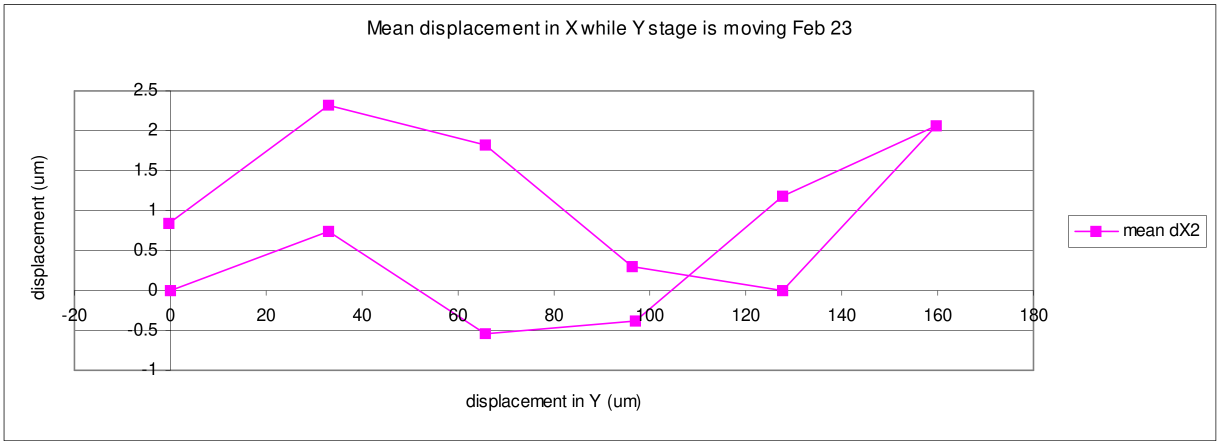


Fig. 8: An example of the tests being carried out to characterize the interactions between motions of the CCD detector.

## 4. SUMMARY AND PROJECT STATUS

All of the major components of GMOS have been completed and now being integrated together in Edinburgh. Extensive tests of the optics and of the individual mechanisms have been carried out to ensure that they meet specifications. All of these components, together with their control software, are expected to be completely integrated together by June, 2000. Figure 9 shows the postfocal plane assembly on an air pallet, waiting for the camera and CCD assembly to be installed.

Fig. 9: The post-focal plane assembly in the cold room testing facility. The grating turret and filter wheels are at the left. The camera barrel will be inserted into the holes in the foreground. This photo should be compared with the drawing in figure 4.

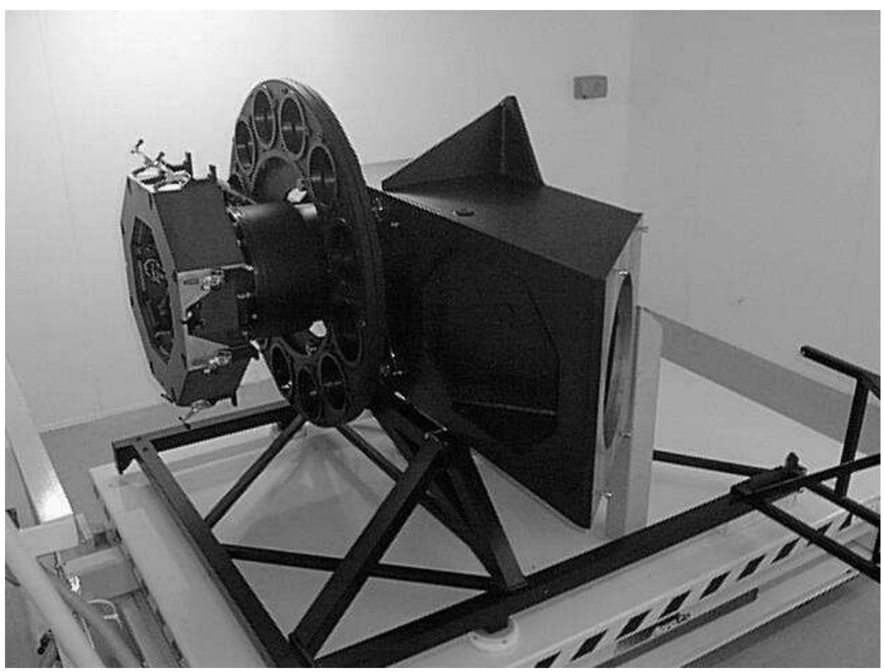

Final testing of the first GMOS instrument will begin immediately after the integration is complete. These tests will include operation and flexure testing in all orientations and temperature conditions expected on the Mauna Kea telescope. Based on the results so far, it is anticipated that GMOS N will be ready for commissioning on the telescope before the end of the year. Components for the GMOS S instrument are nearly all complete and it is anticipated that it will follow about one year later than the Gemini N instrument.

## ACKNOWLEDGMENTS

We thank all the GMOS team members in Durham, Edinburgh and Victoria, who have contributed, and continue to contribute, to the success of this project:

## REFERENCES

1. J. Oschmann "Gemini Project Update", *Gemini newsletter*, 19, 3, 1999.
2. R. L. Davies, et al. "GMOS: The GEMINI Multiple Object Spectrographs", *SPIE* 2871, pp. 1099 – 1106, 1996.
3. R. Murowinski, et al. "The GEMINI Multiobject Spectrographs", *SPIE*, 3355, 297, 1998
4. J.R.Stilburn "High-efficiency sol-gel antireflection coatings for refractive optics", SPIE, this conference
5. K. Szeto, et al. "Gemini Multiobject Spectrograph: a flexure critical design", SPIE 3355, pp. 297 – 306, 1998
6. S. Roberts et al. "Opto-mechanical design of the Gemini Multi-Object Spectrograph On-Instrument Wavefront Sensor, *SPIE* 3132, 1997
7. P. Hastings "Focus and translation mechanisms for the Gemini Multi-Object Spectrograph (GMOS)", *SPIE* 2871, pp. 1216 – 1221, 1996